Some Notes on Tevatron Beam Lifetimes and Longitudinal Emittance

M. Syphers

December 1, 2004

Contents

Introduction

Following the shutdown of the Tevatron complex last year, much improvement was made to the luminosity of the Tevatron Run II Collider program. Before the shutdown it was common for $\sim$20% of each of the two particle beams to be lost during the injection and acceleration processes, often due to poor beam lifetime at injection. After the shutdown, much of this loss was reduced, and hence luminosities increased by $1/(0.8)^2 - 1 = 50\text{-}60\%$, or from typical values of 40×10^{30} cm^{-2}sec^{-1} to values like $60\text{-}70 \times 10^{30}$ cm^{-2}sec^{-1} (along with increased operational stability). Many factors led to the increased luminosity, but a large portion has to be attributed to the fact that a realignment of the Tevatron magnets opened up the transverse aperture, and at the same time the transverse beam size was reduced by better optical matching at injection and by smaller longitudinal emittances – which affect the transverse beam size as well – delivered from the injector chain.

The original purpose of this note was to point out the importance of the longitudinal emittance on perhaps seemingly unrelated transverse effects. Since its inception, the note has also evolved

into a source of hopefully useful information regarding beam distributions and simple diffusion. We start with some basic background of buckets and bunches and longitudinal emittance. We note how the beam size at injection (obviously, horizontal most notably) is dominated by the dispersed orbits due to the momentum spread of the beam. This also leads to the fact that RF noise and longitudinal emittance growth can dominate the growth rate of the transverse beam size and hence beam lifetimes. We discuss a simple model of emittance growth from diffusion, and use this to gain insight into the measured lifetimes and growth rates found in the Tevatron. This note does not provide answers for how to improve the operation of the Tevatron. There are many issues to be solved, such as the source of longitudinal emittance growth leading to DC beam and detector backgrounds. It is hoped, however, that perhaps it will help send some readers (maybe one?) in the right direction, as well as provide some documentation of useful information.

1 Some Useful Relationships for Stationary Buckets

From the equations of motion governing synchrotron oscillations within a stationary bucket[1], the resulting first integral of the motion which relates energy deviation $\Delta E = E - E_s$ with phase can be written as

$$(\Delta E/E_s)^2 - 2\beta^2 \frac{eV}{2\pi h \eta E_s} \cos\phi = constant$$

where the slip factor $\eta = \gamma^{-2} - \gamma_t^{-2}$ is taken to be positive and the phase ϕ is measured relative to the synchronous phase. (For stability with positive η the synchronous phase will be 180°, that is to say, the RF wave passes through zero with a negative slope when $\phi = 0$.) When we speak of the transverse beam size in a synchrotron the momentum spread contributes through the dispersion function, and so we re-write the above in terms of the relative momentum deviation, $\delta \equiv \Delta p/p$,

$$\delta^2 - \frac{1}{2}k^2 \cos\phi = constant$$

where

$$k \equiv \sqrt{\frac{2eV}{\pi h \eta \beta^2 E_s}}.$$

Finally, evaluating the constant in terms of the maximum extent of the momentum oscillation, $\hat{\delta}$,

$$\delta^2 + k^2 \sin^2(\phi/2) = \hat{\delta}^2. \tag{1}$$

The relevant parameters are depicted in Figure 1. Here, the horizontal axis is phase angle $\phi = \omega_{rf}\Delta t$ and the vertical axis is relative momentum deviation $\delta = \Delta p/p = (\Delta E/E_s)/\beta^2$. The trajectory of the stable phase space boundary, or separatrix, is given by $\delta = \pm k\cos(\phi/2)$, from which we see that the parameter k is the "bucket height." The area of the "bucket" in these coordinates is given by $A = 8k$. The bucket area in more conventional energy-time units of eV-sec is found from

$$\mathcal{A} = \beta^2 E_s/\omega_{rf} \cdot 8k = \frac{8\beta^2}{\pi f_{\rm rf}} \sqrt{\frac{E_s eV}{2\pi h \eta \beta^2}}.$$

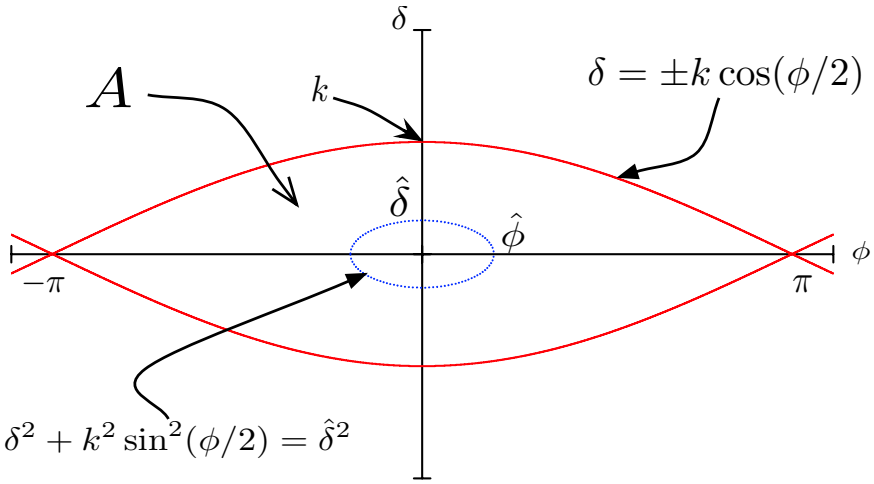

Figure 1: **Stationary bucket in δ - ϕ space.**

Likewise, if given $\mathcal{A}$ in eV-sec, one can compute the maximum momentum deviation from

$$k = \frac{2\pi f_{\rm rf}}{8\beta^2 E_s} \cdot \mathcal{A}.$$

The figure shows also a typical trajectory corresponding to Equation 1. The phase space area bounded by this trajectory is

$$\begin{aligned} 4\int_0^{\hat{\phi}} \left[\hat{\delta}^2 - k^2\sin^2(\phi/2)\right]^{1/2} d\phi &= 8\hat{\delta}\int_0^{\hat{\phi}/2} \sqrt{1-(k/\hat{\delta})^2\sin^2 x}\ dx \\ &= 8\hat{\delta}\ \mathrm{E}(\ \sin^{-1}(\hat{\delta}/k),\ k/\hat{\delta}\ ) \end{aligned}$$

where $\mathrm{E}(x,y)$ is the elliptic integral of the second kind. Note, when $\hat{\delta} = k$, and hence $\hat{\phi} = \pi$, then this area $= 8k\ \mathrm{E}(\pi/2, 1) = 8k = A$.

For small phase angles, the phase space trajectories reduce to ellipses of the form

$$\delta^2 + \left(\frac{k}{2}\phi\right)^2 = \hat{\delta}^2, \qquad \phi \ll 1 \tag{2}$$

with phase space areas $\pi\hat{\phi}\hat{\delta} = \pi k\hat{\phi}^2/2 = 2\pi\hat{\delta}^2/k$. [Note that $\hat{\phi} = 2\hat{\delta}/k$.]

We often talk about the longitudinal emittance of a beam with Gaussian phase and momentum distributions. This description is only valid when the distribution is well within the bucket, i.e., when all phase angles are small. The emittance of a beam is typically defined as the phase space area which encompasses some fraction (95%, for example) of the particles. So, consider a pair of phase space coordinates, x and y, and a set of ellipses with semi-major axes along the x and

y directions with common eccentricity $e = \hat{y}/\hat{x}$. Suppose each ellipse is populated such that the projection onto either the x or y axis is a Gaussian distribution. Then the contour which contains 95% of the particles of such a bi-Gaussian distribution with standard deviations σ_x and σ_y will have an area which is approximately (to about 0.1%) $6\pi\sigma_x\sigma_y = 6\pi e\sigma_x^2 = 6\pi\sigma_y^2/e$.

In our case, the phase space ellipse which contains 95% of the distribution will have

$$area = \frac{12\pi}{k}\sigma_\delta^2 \quad = 3\pi k\sigma_\phi^2.$$

Again, in the more familiar energy-time phase space, the 95% longitudinal emittance, in eV-sec, is given by

$$S = \frac{6\beta^2 E_s}{f_{\rm rf}}\,\frac{1}{k}\,\sigma_\delta^2 \quad = \quad \frac{3\beta^2 E_s}{2f_{\rm rf}}\,k\,\sigma_\phi^2, \qquad S \ll \mathcal{A}$$

for a Gaussian bunch.

2 Measurable Quantities of Some Simple Distributions

As presented above, formulas for emittance are often developed assuming Gaussian distributions, though the actual particle distribution may be far from Gaussian. Due to random events during the course of a particle's life in the accelerator, the Central Limit Theorem dictates that distributions will tend toward Gaussian shapes. However, this can often take some time especially for hadron beams, and processes like coalescing several bunches into one, for example, can produce much more complicated distributions. For this reason, it is sometimes convenient to think of emittances in terms of moments of the distribution, which are more easily measured directly, rather than atttempting to "fit" a parameter, such as the standard deviation σ_x of a presumed Gaussian curve, to a specific distribution measurement of the variable x. To this end we will think of emittances in terms of the second moment of the particle distribution, noting that for a pure Gaussian distribution the variance, $\sigma_x^2 = \langle x^2\rangle \equiv x_{rms}^2$, *is* the second moment.

In what follows we compare the rms relative momentum deviation and rms phase angle (and time spread) between three different simple beam distributions: (a) a Gaussian bunch, for $S \ll \mathcal{A}$, (b) a uniformly populated bunch, for $\epsilon_L \ll \mathcal{A}$, and (c) and a uniformly populated (full) bucket. Much more thorough discussions of general longitudinal distributions may be found in the literature.[2]

(a) Gaussian Bunch

The results for a Gaussian bunch are quoted at the end of the last section, but are re-written here with the 95% longitudinal emittance, $S \ll \mathcal{A}$, as an input parameter:

$$\delta_{rms} = \sqrt{\frac{kf_{\rm rf}S}{6\beta^2 E_s}} \tag{3}$$

$$\phi_{rms} = \sqrt{\frac{2f_{\rm rf}S}{3k\beta^2 E_s}} \tag{4}$$

The particle density function, normalized to a single particle, is familiar:

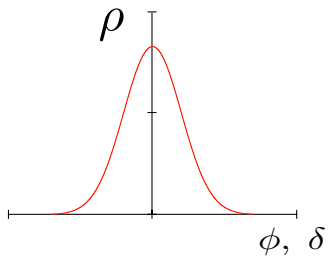

$$\rho(\phi,\delta) = \frac{1}{\sqrt{2\pi}\phi_{rms}} \exp(-\phi^2/2\phi_{rms}^2) \times \frac{1}{\sqrt{2\pi}\delta_{rms}} \exp(-\delta^2/2\delta_{rms}^2).$$

Figure 2: **Gaussian distribution.**

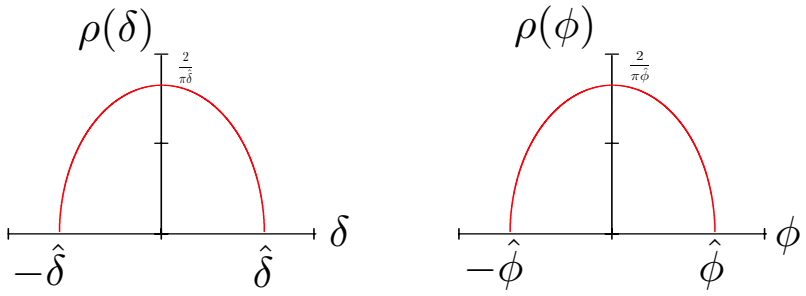

Figure 3: **Distribution functions for uniform bunch with $\epsilon_L \ll \mathcal{A}$.**

(b) Uniform Bunch

Next, consider a bunch for which 100% of the particles uniformly populate a phase space ellipse with maxima $\hat{\phi}$ and $\hat{\delta}$. The area of the ellipse is $\pi\hat{\delta}\hat{\phi}$. The particle density function is then

$$\rho(\phi,\delta) = \frac{1}{\pi\hat{\phi}\hat{\delta}}$$

The phase space trajectories are ellipses given by Equation 2, and so the distributions along ϕ and along δ are given by

$$\begin{aligned} \rho(\phi) &= \frac{2}{\pi\hat{\phi}\hat{\delta}} \int_0^{\sqrt{1-\phi^2/\hat{\phi}^2}} d\delta \\ &= \frac{2}{\pi\hat{\phi}} \sqrt{1-\phi^2/\hat{\phi}^2}, \qquad \textit{and} \\ \rho(\delta) &= \frac{2}{\pi\hat{\delta}} \sqrt{1-\delta^2/\hat{\delta}^2} \end{aligned}$$

as depicted in Figure 3. The rms of each projection can be found by taking

$$\langle\phi^2\rangle = \frac{1}{\pi\hat{\delta}\hat{\phi}} \int_{-\hat{\phi}}^{\hat{\phi}} \int_{-\hat{\delta}\sqrt{1-(\phi/\hat{\phi})^2}}^{\hat{\delta}\sqrt{1-(\phi/\hat{\phi})^2}} \phi^2\, d\delta\, d\phi$$

$$= \hat{\phi}^2 \frac{2}{\pi} \int_{-1}^{1} \sqrt{1-u^2}\, u^2 du$$
$$= \hat{\phi}^2/4$$

or,

$$\phi_{rms} = \frac{1}{2}\hat{\phi}, \qquad \text{and, similarly,} \qquad \delta_{rms} = \frac{1}{2}\hat{\delta}.$$

In terms of energy-time coordinates, where 100% of the particles are contained within an ellipse of area ϵ_L, given in eV-sec, these quantities are

$$\phi_{rms} = \sqrt{\frac{\epsilon_L f_{\rm rf}}{\beta^2 E_s}\,\frac{1}{k}}, \qquad \delta_{rms} = \sqrt{\frac{\epsilon_L f_{\rm rf}}{\beta^2 E_s}\,\frac{k}{4}}$$

(c) Uniform Bucket

Lastly, we examine an RF bucket which is entirely populated uniformly with particles. First, we look at the projections along ϕ and δ and their rms values. The density function is $\rho(\phi,\delta) = 1/A$ and so upon integrating over δ we get

$$\rho(\phi) = \frac{1}{A}\int_{-k\cos\phi/2}^{k\cos\phi/2} d\delta = \frac{2k}{A}\cos(\phi/2) = \frac{1}{4}\cos(\phi/2)$$

which is plotted in Figure 4.

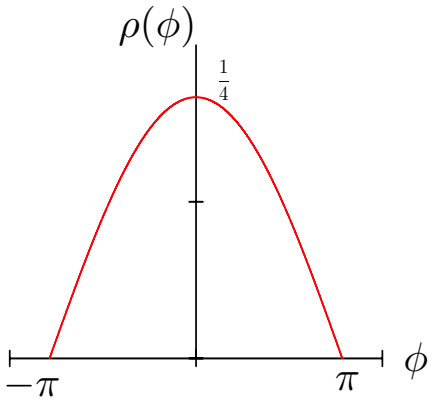

Figure 4: **Phase distribution function for uniformly filled bucket.**

We then find the variance of the phase angle,

$$\langle\phi^2\rangle = \frac{1}{4}\int_{-\pi}^{\pi} \phi^2 \cos(\phi/2) d\phi = 4\int_0^{\pi/2} x^2 \cos x\, dx$$

$$
\begin{aligned}
&= 4\left[(x^2\sin x)|_0^{\pi/2} - 2\int_0^{\pi/2} x\sin x\; dx\right] \\
&= \pi^2 - 8
\end{aligned}
$$

and so,

$$\phi_{rms} = \pi\sqrt{1-\frac{8}{\pi^2}} = 0.435\;\pi.$$

Note that the measured bunch length in units of time will be

$$\Delta t_{rms} = \frac{0.435}{2f_{\rm rf}}.$$

Repeating the process by first integrating over phase angles,

$$\rho(\delta) = \frac{1}{\mathcal{A}}\int_{-2\cos^{-1}(|\delta|/k)}^{2\cos^{-1}(|\delta|/k)} d\phi = \frac{1}{8k}\cdot 2\cdot[2\cos^{-1}(|\delta|/k)] = \frac{1}{2k}\cos^{-1}(|\delta|/k)$$

which is plotted in Figure 5.

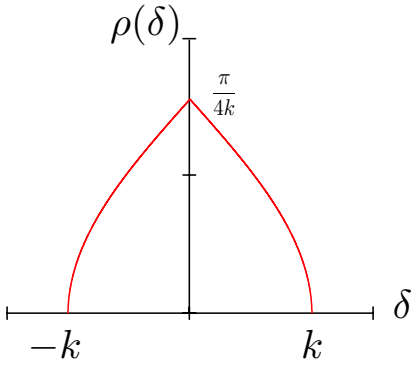

Figure 5: **Relative momentum distribution function for uniformly filled bucket.**

Integrating to find the variance of the momentum distribution,

$$
\begin{aligned}
\langle\delta^2\rangle &= \frac{1}{2k}\int_{-k}^{k}\cos^{-1}(|\delta|/k)\;\delta^2 d\delta \\
&= \frac{1}{k}\int_0^k \delta^2\cos^{-1}(\delta/k)d\delta = k^2\int_0^1 x^2\cos^{-1}x\;\; dx \\
&= \frac{2}{9}k^2
\end{aligned}
$$

and so,

$$\delta_{rms} = \frac{\sqrt{2}k}{3}.$$

Summary

Summarizing the above discussion, we define

$$\begin{array}{rcl} \mathcal{A} & = & \text{bucket area} \\ S & = & 95\% \text{ emittance of Gaussian bunch, with } S \ll \mathcal{A} \\ \epsilon_L & = & 100\% \text{ emittance of uniformly populated bunch, with } \epsilon_L \ll \mathcal{A} \end{array}$$

with all quantities above in energy-time units, eV-sec, say. Then the bucket height is

$$k \;=\; \sqrt{\frac{2eV}{\pi h \eta \beta^2 E_s}} \;=\; \frac{\pi f_{\rm rf} \mathcal{A}}{4\beta^2 E_s},$$

and the bucket area is

$$\mathcal{A} \;=\; \frac{4\beta^2 E_s k}{\pi f_{\rm rf}} \;=\; \frac{8\beta^2}{\pi f_{\rm rf}} \sqrt{\frac{E \cdot eV}{2\pi h \eta \beta^2}}.$$

Then, for the case of a Gaussian bunch, with longitudinal emittance S, with $S \ll \mathcal{A}$, we find

$$\begin{aligned} \delta_{rms} &= \sqrt{\frac{S f_{\rm rf}}{6\beta^2 E_s} \cdot k} \;=\; \left(\frac{f_{\rm rf}\mathcal{A}}{\beta^2 E_s}\right) \sqrt{\frac{\pi}{24}\left(\frac{S}{\mathcal{A}}\right)} \\ \phi_{rms} &= \sqrt{\frac{2S f_{\rm rf}}{3\beta^2 E_s} \cdot \frac{1}{k}} \;=\; \sqrt{\frac{8}{3\pi}\left(\frac{S}{\mathcal{A}}\right)} \end{aligned}$$

whereas for a Uniform bunch, with 100% longitudinal emittance $\epsilon_L \ll \mathcal{A}$, we find

$$\begin{aligned} \delta_{rms} &= \sqrt{\frac{\epsilon_L f_{\rm rf}}{4\beta^2 E_s} \cdot k} \;=\; \left(\frac{f_{\rm rf}\mathcal{A}}{\beta^2 E_s}\right) \sqrt{\frac{\pi}{16}\left(\frac{\epsilon_L}{\mathcal{A}}\right)} \\ \phi_{rms} &= \sqrt{\frac{\epsilon_L f_{\rm rf}}{\beta^2 E_s} \cdot \frac{1}{k}} \;=\; \sqrt{\frac{4}{\pi}\left(\frac{\epsilon_L}{\mathcal{A}}\right)} \quad . \end{aligned}$$

For a filled, uniformly populated bucket, we get

$$\begin{aligned} \delta_{rms} &= \frac{\sqrt{2}}{3} \cdot k \;=\; \left(\frac{f_{\rm rf}\mathcal{A}}{\beta^2 E_s}\right) \left(\frac{\pi\sqrt{2}}{12}\right) \\ \phi_{rms} &= \pi\sqrt{1 - \frac{8}{\pi^2}} \;=\; 0.435\,\pi. \end{aligned}$$

Putting in some relevant numbers for the Tevatron, we take $f_{\rm rf} = 53$ MHz, $\eta = 1/18^2$, $h = 1113$, $eV = 1$ MeV, and $\beta = 1$ and examine the above quantities for beam energies of 150 GeV and 1000 GeV. We look at cases where S and $\epsilon_L = 2$ eV-sec, since this is a typical value upon injection from the Main Injector. The results are tabulated below in Table 1.

Table 1: Tevatron parameters applied to expressions above.

	$E =$	150	1000	GeV
	$k =$	1.1	0.43	10^{-3}
	$\mathcal{A} =$	4.0	10	eV-sec
	$f_{\rm rf}\mathcal{A}/\beta^2 E_s =$	1.42	0.55	10^{-3}
Gaussian, with				
$S = 2$ eV-sec (95%):	$S/\mathcal{A} =$	0.5	0.2	
	$\delta_{rms} =$	0.36	0.087	10^{-3}
	$\phi_{rms} =$	0.21	0.13	π
	$\Delta\tau_{rms} =$	2.0	1.2	nsec
Uniform, with				
$\epsilon_L = 2$ eV-sec (100%):	$\epsilon_L/\mathcal{A} =$	0.5	0.2	
	$\delta_{rms} =$	0.44	0.11	10^{-3}
	$\phi_{rms} =$	0.25	0.16	π
	$\Delta\tau_{rms} =$	2.4	1.5	nsec
Uniform,				
full bucket:				
	$\delta_{rms} =$	0.52	0.20	10^{-3}
	$\phi_{rms} =$	0.44	0.44	π
	$\Delta\tau_{rms} =$	4.1	4.1	nsec

3 Momentum Contributions to Transverse Beam Size

Consider a distribution of particles undergoing betatron oscillations as observed at a point where the amplitude function has value β_0. Relative to the closed orbit, the oscillations have zero mean and an rms spread $\langle x_\beta^2 \rangle^{1/2}$. If the closed orbit itself is determined by the momentum of the particle through the value of the dispersion function D at this point in the synchrotron, then the total displacement of a particle relative to the ideal trajectory (for the central momentum) is

$$x = x_\beta + D\ \delta$$

and taking the square and averaging over the particles we get

$$\begin{aligned} x^2 &= x_\beta^2 + 2x_\beta D\delta + D^2\ \delta^2 \\ \langle x^2 \rangle &= \langle x_\beta^2 \rangle + 2\langle x_\beta \rangle D\langle \delta \rangle + D^2\ \langle \delta^2 \rangle \\ &= \langle x_\beta^2 \rangle + D^2\ \langle \delta^2 \rangle. \end{aligned}$$

Here we have made no assumptions about the distributions in betatron amplitudes or in relative momentum deviation – they are not necessarily Gaussian. We only assume that the momentum and betatron oscillation amplitudes are uncorrelated and each distribution has zero mean.

Let's look at the total beam size at a typical ring location in the Tevatron. If the 95% normalized transverse emittance, ϵ_n, is defined by

$$\epsilon_n \equiv \frac{6\pi \langle x_\beta^2 \rangle}{\beta_0}\ (\beta\gamma)$$

then the variance of the transverse particle distribution is

$$\langle x^2 \rangle = \frac{\beta_0 \epsilon_n}{6\pi(\beta\gamma)} + D^2 \langle \delta^2 \rangle.$$

Consider the following two cases: (a) Injection conditions in the Tevatron, with a full, uniform bucket (4 eV-sec) at 150 GeV and 20π mm-mrad transverse emittance, and (b) Collision conditions (1000 GeV) in the Tevatron for a Gaussian 4 eV-sec bunch with 20π mm-mrad transverse emittance. Then the relative contributions to the beam size at a typical cell location, with $\beta_0 = 100$ m and $D = 4$ m, are:

$$x_{rms}^2 = \frac{\epsilon_n \beta_0}{6\pi(\beta\gamma)} + D^2 \langle \delta^2 \rangle$$

$$\begin{aligned} \text{(a) injection}: \quad x_{rms}^2 &= \frac{(20\pi)(100)}{6\pi(160)}\ \text{mm}^2 + (4\ \text{m})^2 (0.5 \times 10^{-3})^2 \\ &= (1.4\ \text{mm})^2 + (2.0\ \text{mm})^2 \\ &= (2.4\ \text{mm})^2 \end{aligned}$$

$$\begin{aligned} \text{(b) collision}: \quad x_{rms}^2 &= \frac{(20\pi)(100)}{6\pi(1000)}\ \text{mm}^2 + (4\ \text{m})^2 (0.12 \times 10^{-3})^2 \\ &= (0.58\ \text{mm})^2 + (0.48\ \text{mm})^2 \\ &= (0.75\ \text{mm})^2 \end{aligned}$$

Note that at 150 GeV, if the transverse emittance shrank to zero, the horizontal beam size would only be reduced by 17%!

At the "17" locations in the Tevatron, where the dispersion function is about 6 m, the momentum contribution to the beam size goes from 2 mm to 3 mm at injection, and from 0.48 mm to 0.72 mm at high energy. The point here is that the typical transverse (horizontal) beam size in the Tevatron is very much dominated by the momentum spread, or longitudinal emittance, at injection and still plays a significant role at high energy.

During a store, the emittances of the beam grow mainly due to diffusion mechanisms, such as beam-gas scattering, RF noise, and so forth. Typical numbers for diffusion rates at 1 TeV tend to be on the scale of 0.5π mm-mrad/hr for transverse, and 0.1-0.5 eV-sec/hr for longitudinal. (The same mechanisms may generate larger effects at 150 GeV.) Let us compare the relative importance of these rates on the rate of increase of the transverse beam size. Denoting the total transverse rms beam size as $\sigma \equiv \langle x^2 \rangle^{1/2}$, we note that

$$\begin{aligned} \frac{d\sigma^2}{dt} &= \frac{\beta_0}{6\pi\beta\gamma}\frac{d\epsilon_n}{dt} + D^2\frac{d}{dt}(\delta_{rms}^2) \\ &= \frac{\beta_0}{6\pi\beta\gamma}\,\dot{\epsilon}_n + D^2\left(\frac{kf_{\rm rf}}{6\beta^2 E_s}\right)\,\dot{S} \end{aligned}$$

where, in the above, we have assumed a Gaussian bunch with $S \ll \mathcal{A}$. Plugging in Tevatron parameters at (a) injection, and (b) high energy, we find

$$\frac{d\sigma^2}{dt} = \frac{\beta_0}{6\pi\beta\gamma}\,\dot{\epsilon}_n + \left(\frac{kf_{\rm rf}D^2}{6\beta^2 E_s}\right)\,\dot{S}$$

$$\begin{aligned} \text{(a)} &= \frac{100}{6(160)}\left(\frac{\dot{\epsilon}_n}{\pi\ \text{mm}\cdot\text{mrad/hr}}\right)\frac{\text{mm}^2}{\text{hr}} + \left(\frac{(10^{-3})(53\times10^6)(4^2)}{6\cdot150\times10^9}\right)\left(\frac{\dot{S}}{\text{eV}\cdot\text{sec/hr}}\right)\frac{\text{mm}^2}{\text{hr}} \\ &\approx \frac{1}{10}\left(\frac{\dot{\epsilon}_n}{\pi\ \text{mm}\cdot\text{mrad/hr}}\right)\frac{\text{mm}^2}{\text{hr}} + \ 1\ \left(\frac{\dot{S}}{\text{eV}\cdot\text{sec/hr}}\right)\frac{\text{mm}^2}{\text{hr}} \end{aligned}$$

$$\begin{aligned} \text{(b)} &= \frac{100}{6(1066)}\left(\frac{\dot{\epsilon}_n}{\pi\ \text{mm}\cdot\text{mrad/hr}}\right)\frac{\text{mm}^2}{\text{hr}} + \left(\frac{(0.4\cdot10^{-3})(53\cdot10^6)(4^2)}{6\cdot1000\times10^9}\right)\left(\frac{\dot{S}}{\text{eV}\cdot\text{sec/hr}}\right)\frac{\text{mm}^2}{\text{hr}} \\ &\approx \frac{1}{60}\left(\frac{\dot{\epsilon}_n}{\pi\ \text{mm}\cdot\text{mrad/hr}}\right)\frac{\text{mm}^2}{\text{hr}} + \ \frac{1}{20}\ \left(\frac{\dot{S}}{\text{eV}\cdot\text{sec/hr}}\right)\frac{\text{mm}^2}{\text{hr}}. \end{aligned}$$

The above tells us that (a) at injection, a growth rate of $\dot{S} = 0.1$ eV-sec/hr has the same contribution to the rate of increase in beam size as a growth rate of $\dot{\epsilon}_n = 1\ \pi$ mm-mrad/hr, and (b) at high energy, rates of $\dot{S} = 0.3$ eV-sec/hr and $\dot{\epsilon}_n = 1\ \pi$ mm-mrad/hr have comparable effects.

From the previous pages, it should be no surprise when beam loss seen in the Tevatron is highly correlated with longitudinal emittance and beam lifetimes are correlated with its growth rate.

4 Growth Rates and Beam Lifetimes due to Simple Diffusion

A long beam lifetime does not imply that there is no emittance growth happening, and likewise emittance growth does not imply a short beam lifetime. The important quantities, of course, are the ratio of the emittance growth rate relative to the admittance (aperture, if you like) of the accelerator and the initial beam size. A simple diffusion model can suffice to show the interplay between emittance growth rate and beam lifetime. We will follow roughly the notation in Chapter 7 of [1].

First, define a single particle emittance $\epsilon_p \equiv r^2$, where r is an amplitude in phase space. For transverse motion, we should identify $r^2 = [x^2 + (\beta x' + \alpha x)^2]/\beta$. For our discussion above, $r^2 = [\delta^2 + (k\phi/2)^2]/(k/2)$, for instance. But for the present discussion, let's simplify by letting $r^2 = x^2 + y^2$, where x and y form an appropriate set of arbitrary phase space variables.

Next, define $Z = \epsilon_p/W$, where W is the admittance of the accelerator, that is, the maximum phase space area beyond which the particle is lost. The effective aperture of the accelerator is at $r = a$, where $W = a^2$, or where $Z = 1$. We assume that the coordinates are chosen, as in our examples above, such that the initial phase space distribution is cylindrically symmetric.

Finally, define an emittance growth rate, or diffusion rate, R, given by

$$R \equiv \frac{d}{dt}\langle r^2 \rangle = \frac{d}{dt}\langle \epsilon_p \rangle.$$

Note: $R = 2\ d\langle x^2 \rangle/dt$.

The 2-D diffusion equation governing how the distribution function $f(r,t)$ varies with position and time is

$$\frac{\partial f}{\partial t} = \frac{R}{4}\nabla^2 f = \frac{R}{4}\ \frac{1}{r}\frac{\partial}{\partial r}\left(r\frac{\partial f}{\partial r}\right)$$

or, in terms of ϵ_p and t,

$$\frac{\partial f}{\partial t} = R\frac{\partial}{\partial \epsilon_p}\left(\epsilon_p \frac{\partial f}{\partial \epsilon_p}\right).$$

We can simplify the treatment by introducing the new dimensionless variable, $\tau \equiv (R/W)\ t$ and write

$$\frac{\partial f}{\partial \tau} = \frac{\partial}{\partial Z}\left(Z\frac{\partial f}{\partial Z}\right)$$

and we note that the constraints on the problem are the form of the initial distribution, which we will assume only depends upon r or Z [that is, $f(Z,0) = f_0(Z)$], and the fact that the distribution goes to zero at the aperture for all time: $f(1,\tau) = 0$.

The solution of the above differential equation subject to the given boundary conditions is

$$f(Z,\tau) = \sum_n c_n J_0(\lambda_n \sqrt{Z}) e^{-\lambda_n^2 \tau/4}$$

where

$$c_n = \frac{1}{J_1(\lambda_n)^2} \int_0^1 f_0(Z) J_0(\lambda_n \sqrt{z}) dZ \tag{5}$$

and λ_n is the n-th zero of the Bessel function $J_0(x)$. The first zero is $\lambda_1 \approx 2.405$, for example.

The above seems like a lot of running around, so let's try to get to the payoff. From the above solution, we can immediately write down how the beam distribution will vary with time (τ), how its rms – and hence the emittance – will vary, how the beam intensity will vary with time, and therefore how the instantaneous beam lifetime will evolve.

Intensity vs. Time

$$\begin{aligned} N(\tau) &= \int_0^1 f(Z,\tau) dZ \\ &= 2 \sum_n \frac{c_n}{\lambda_n} J_1(\lambda_n) e^{-\lambda_n^2 \tau/4} \end{aligned} \tag{6}$$

Lifetime vs. Time

$$\begin{aligned} \tau_L &\equiv -\frac{N(\tau)}{dN/d\tau} \\ &= \frac{4 \sum (c_n/\lambda_n) J_1(\lambda_n) e^{-\lambda_n^2 \tau/4}}{\sum c_n \lambda_n J_1(\lambda_n) e^{-\lambda_n^2 \tau/4}} \\ &\to \frac{4}{\lambda_1^2} = \frac{4}{(2.405)^2} = 0.692 \qquad \text{as } t \to \infty \end{aligned}$$

Particle Distribution vs. Time

$$\begin{aligned} f(Z,\tau) &= \sum_n c_n J_0(\lambda_n \sqrt{Z}) e^{-\lambda_n^2 \tau/4} \\ \to f^\infty(Z) &= c_1 J_0(\lambda_1 \sqrt{Z}) e^{-\lambda_1^2 \tau/4} \qquad \text{as } t \to \infty \end{aligned}$$

from which we can derive the rms of the equilibrium distribution by first computing

$$\langle Z \rangle^\infty = \frac{\int_0^1 J_0(\lambda_1 \sqrt{Z}) Z dZ}{\int_0^1 J_0(\lambda_1 \sqrt{Z}) dZ} = \frac{\int_0^1 u^3 J_0(\lambda_1 u) du}{\int_0^1 u J_0(\lambda_1 u) du} = 0.308.$$

This tells us that after an adequate amount of time, the distribution will grow toward the aperture and eventually reach an equilibrium state, exponentially decaying away with a lifetime $\tau_L^\infty = 4/\lambda_1^2$, and the variance of the final distribution in phase space coordinate x will be given by

$$\langle x^2 \rangle^\infty = \langle r^2 \rangle^\infty / 2 = W \langle Z \rangle^\infty / 2 = 0.154 \; W = 0.154 \; a^2$$

or,

$$x_{rms}^\infty = \sqrt{0.154} a = 0.393 \; a.$$

Comments

We see that if the distribution is allowed to reach equilibrium, the extent of the effective aperture can be deduced by measuring the rms of the final distribution. Likewise, by measuring the equilibrium beam lifetime, t_L, we see that the diffusion rate can be found from

$$t_L = \tau_L^\infty \cdot \left(\frac{W}{R}\right) = \frac{4}{\lambda_1^2}\left(\frac{W}{R}\right) = \frac{4a^2}{\lambda_1^2 R}.$$

Traditionally at Fermilab, 95% emiitances are "measured" by actually measuring the distribution over a coordinate x, finding the rms, and defining emittance as $\epsilon \equiv 6\pi\langle x^2\rangle$. With this procedure in mind, consider a Gaussian beam, with $\epsilon_i = 6\pi\langle x^2\rangle = 6\pi\sigma_0^2$, where $\sigma_0 \ll a$. Due to a diffusion mechanism, the emittance will grow, the edge of the distribution will reach the aperture and particles will begin to be lost. Eventually, the distribution will reach equilibrium – not Gaussian! – and its measured emittance, keeping with the above definition, will be

$$\epsilon_f = 6\pi\langle x^2\rangle = 0.924\pi\ a^2.$$

Suppose the final lifetime is measured experimentally to be t_L. Then, the emittance growth rate due to the diffusion in the absence of any aperture is

$$\dot{\epsilon} = 6\pi\frac{d\langle x^2\rangle_0}{dt} = 6\pi \cdot R/2 = \frac{12\pi a^2}{\lambda_1^2 t_L} \approx \frac{12\epsilon_f}{(2.405)^2 t_L} \approx 2\epsilon_f/t_L.$$

Allowing the beam distribution to reach equilibrium and subsequently measuring the resulting lifetime and the variance of the final distribution allows one to compute the diffusion rate. This method has been used experimentally in the past to evaluate the performance of various synchrotrons.[3] The final equilibrium distribution, f^∞, is shown in Figure 6 as a function of r. The central part of the distribution appears Gaussian, but deviates near the aperture where it must go to zero.

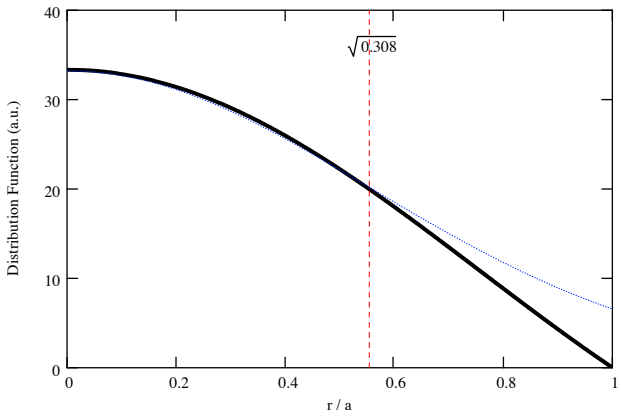

Figure 6: **Equilibrium particle distribution f^∞ as a function of phase space amplitude $r = \sqrt{Z}$. The aperture is at $r = a = 1$. The dotted curve is a Gaussian with the same variance, $\langle r^2\rangle = \langle Z\rangle^\infty = 0.308$, for comparison.**

4.1 Some Numerical Examples

Illustrations of the previous discussion are provided in Figures 7-12. We examine 6 cases. In the first three, the initial beam distribution begins as Gaussian, with standard deviations σ_0, and with effective apertures at radii (a) $a = 10\sigma_0$, (b) $a = 3\sigma_0$, and (c) $a = \sigma_0$. The last three cases involve initial distributions which are uniform out to radii (d) $r = 2a/3$, (e) $r = 5a/6$, and (f) $r = a$. For each case we plot N, τ_L, and $\langle x^2 \rangle$ (i.e., "emittance") as functions of τ.

In case (a), we see that the intensity remains constant as well as the emittance growth rate until the beam reaches the aperture, at which time the beam lifetime drops. For initial distributions with rms much less than the available aperture, the intensity function has an inflection point at around $\tau \approx 0.5$, after which the lifetime approaches its asymptotic limit, as does the emittance.

In case (b), the extent of the beam is essentially equal to the aperture. In fact, a small beam loss at injection, about 1%, is noticeable as the initial beam is clipped. The lifetime, which is initially small due to the immediate loss, quickly increases, but again drops toward $4/\lambda_1^2$. The emittance doesn't have as far to go to reach equilibrium.

In case (c), the beam size is initially much larger than the aperture, and so 60% of the beam is lost immediately. The lifetime is zero, and increases to equilibrium. The emittance, measured as $\langle x^2 \rangle$, actually decreases as the equilibrium distribution is formed.

For the remaining examples, the beam distribution starts out uniform. For a uniform beam with maximum extent much less than the aperture the distribution will soon develop into a Gaussian due to the random diffusion process and the resulting curves will look much like those found in cases (a) through (c). For example, consider a phase space uniform out to a radius which is 1/5 the aperture. Then the rms of the distribution will start out at 1/10 the aperture radius. The final behavior of the intensity curve will look essentially identical to Figure 7 [case (a)]. The defining behavior will become apparent when the extent of the initial distribution is closer to the aperture.

In case (d), the beam is uniform out to a radius $r = 0.67a$. The rms of the distribution is thus 1/3 the aperture. As one might expect, the resulting plots have similar features to those of Figure 8.

In case (e), the beam is uniform out to a radius $r = 0.83a$. The original rms is thus $0.42a$, slightly larger than the equilibrium value of $0.393a$. However, the beam is still entirely within the aperture at first, and so the emittance grows, until the aperture is reached, and then decays away until equilibrium is attained.

Finally, in case (f), the beam is uniform all the way out to the aperture at $r = a$. Case (f) looks very similar to case (c). It should. The center of a Gaussian distribution is essentially uniform, and so the lifetimes and emittance behaviors should look very similar. The difference between these cases is in the intensity plot. Here, the beam is entirely (barely) within the aperture upon injection. Note that during very early times ($\tau \ll 0.1$) the beam intensity evolution is not exponential, but initially appears to fall as $\exp(-\sqrt{t})$. More will be said about this in a subsequent section.

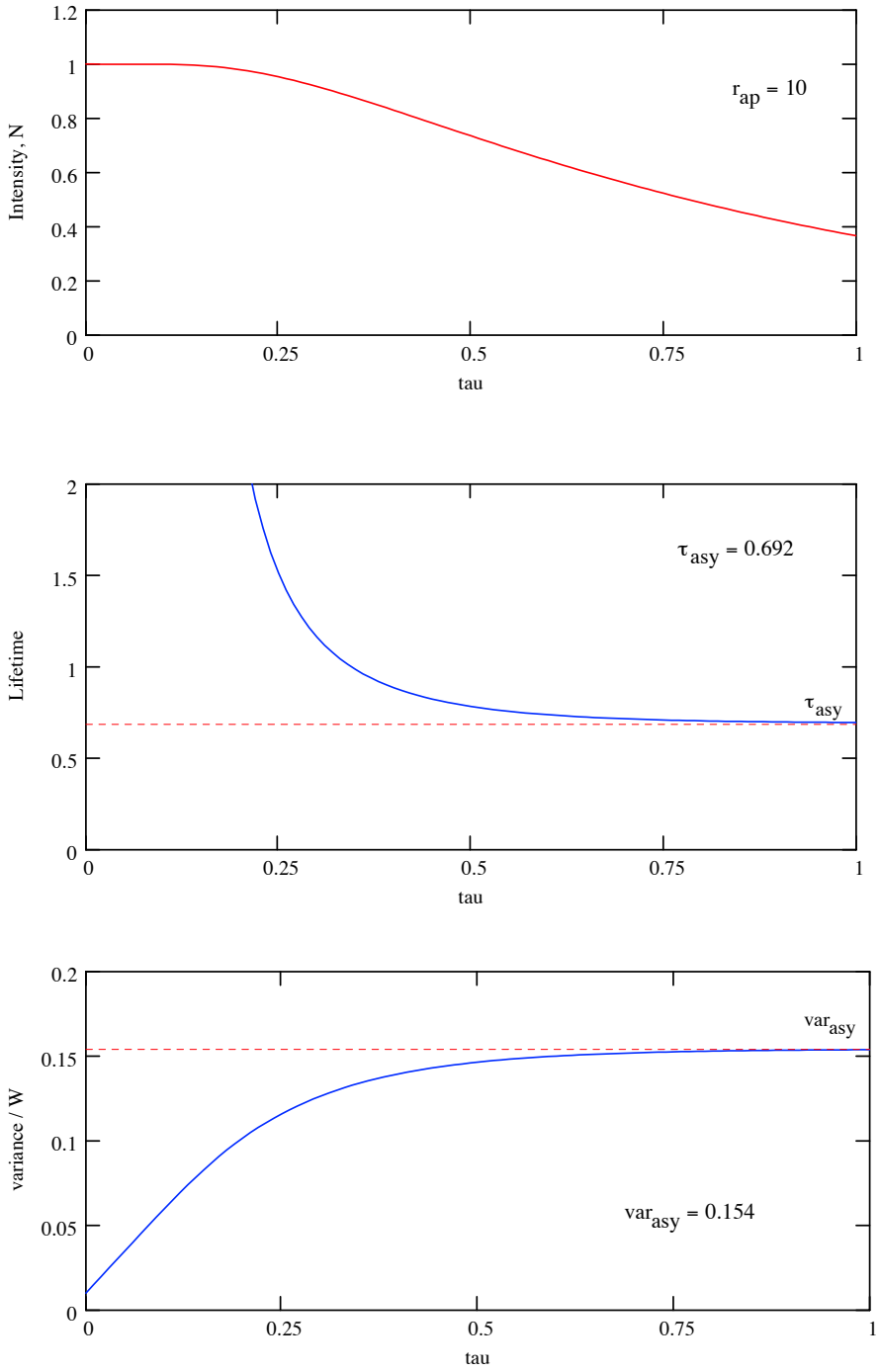

Figure 7: **Case (a) – Top to bottom: intensity N, lifetime τ_L, emittance $\langle x^2\rangle/W$ versus τ. Here, the initial beam distribution was Gaussian, with $\sigma_0 = a/10$.**

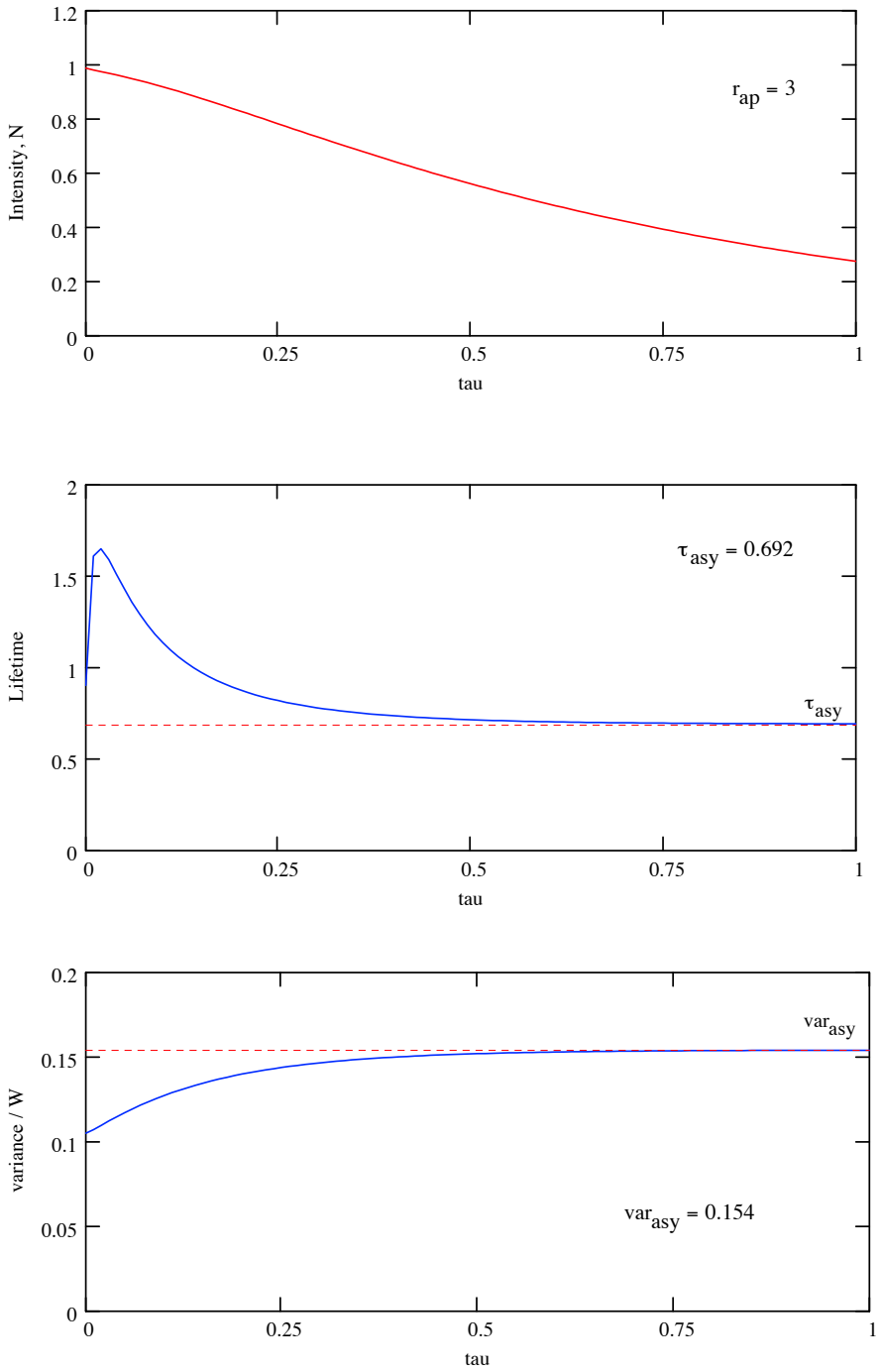

Figure 8: **Case (b) – Top to bottom: intensity N, lifetime τ_L, emittance $\langle x^2\rangle/W$ versus τ. Here, the initial beam distribution was Gaussian, with $\sigma_0 = a/3$.**

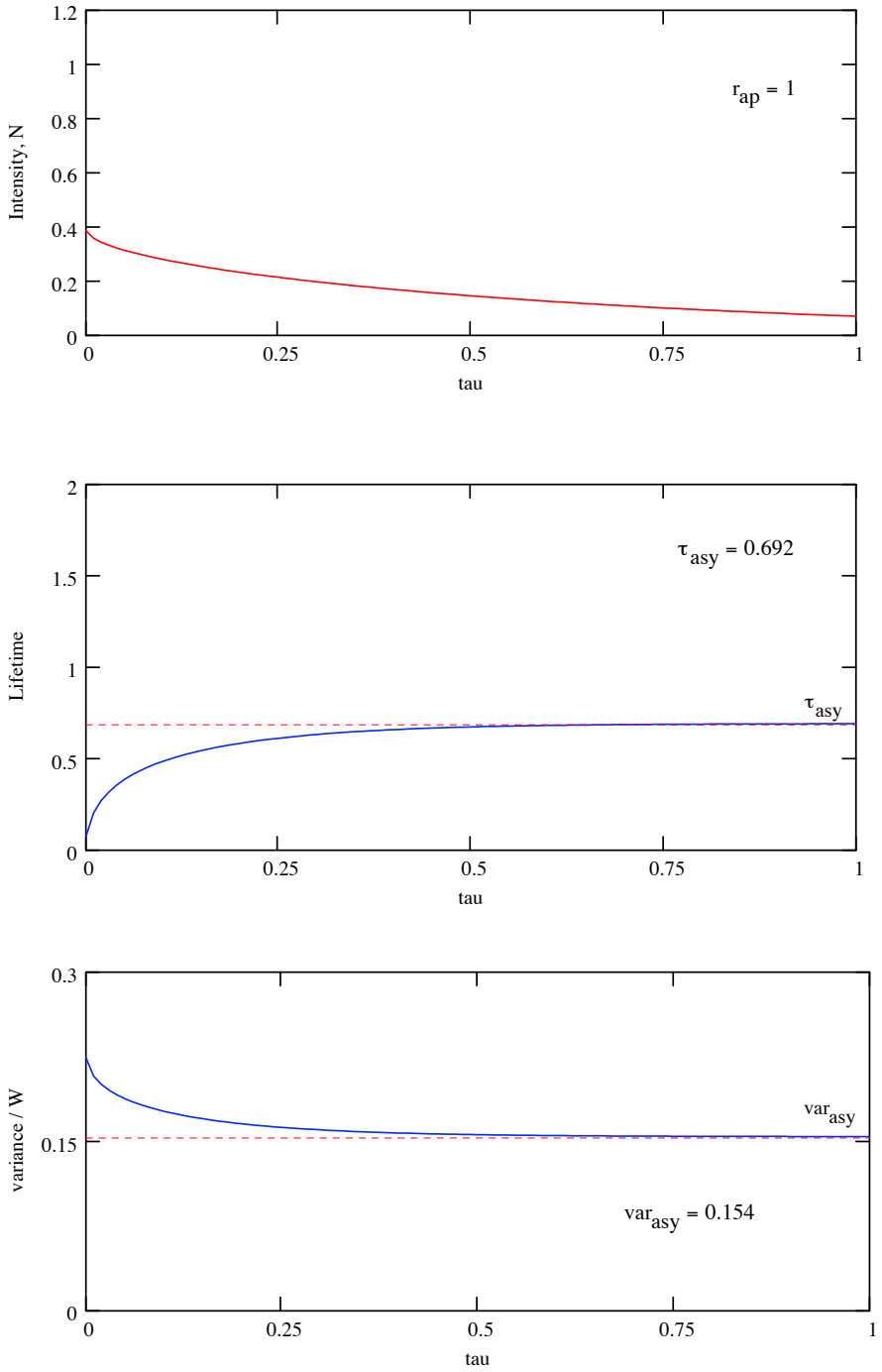

Figure 9: **Case (c) – Top to bottom: intensity N, lifetime τ_L, emittance $\langle x^2\rangle/W$ versus τ. Here, the initial beam distribution was Gaussian, with $\sigma_0 = a$.**

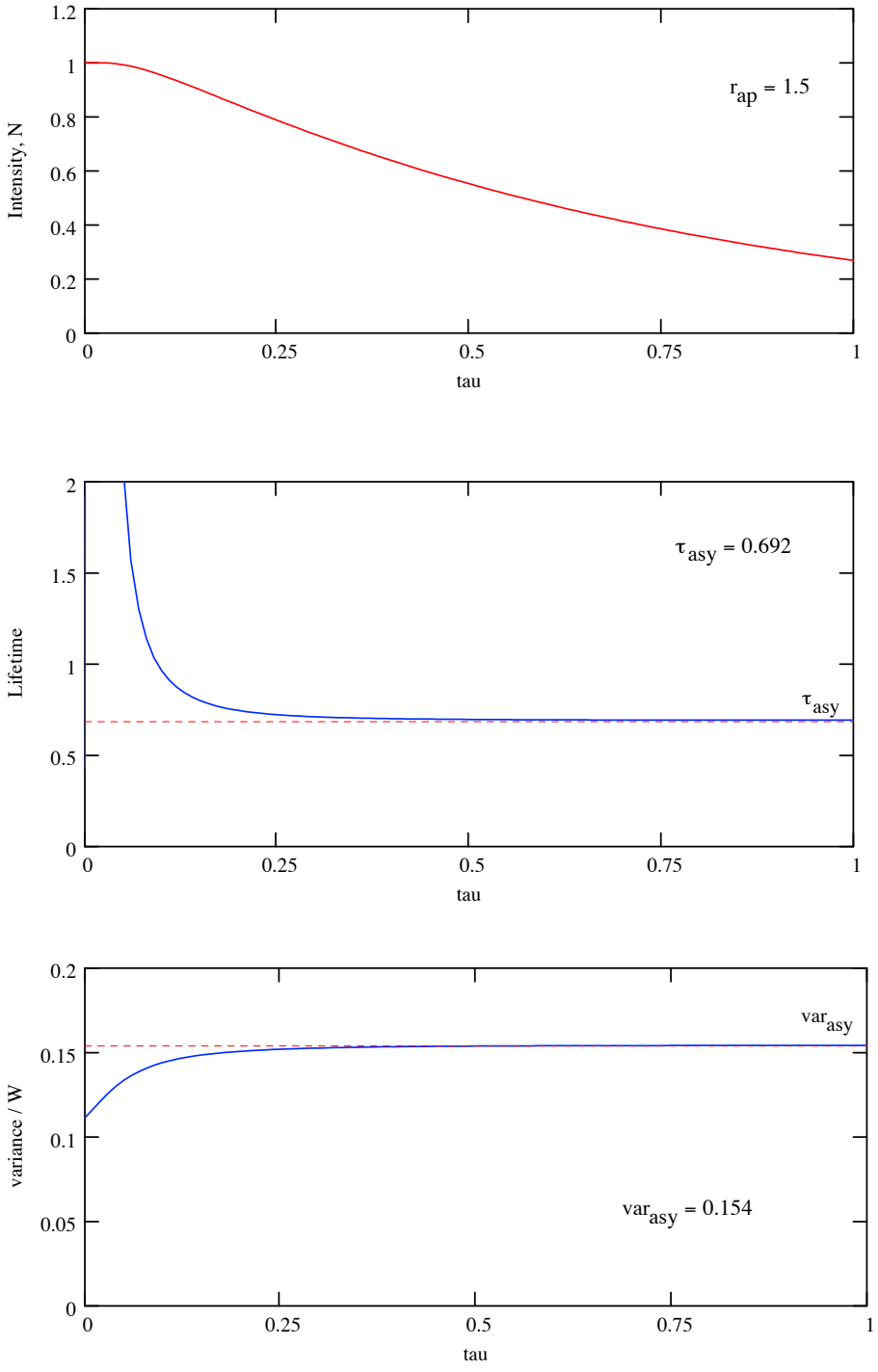

Figure 10: **Case (d) – Top to bottom: intensity N, lifetime τ_L, emittance $\langle x^2 \rangle / W$ versus τ. Here, the initial beam distribution was uniform, out to $r = 2a/3$.**

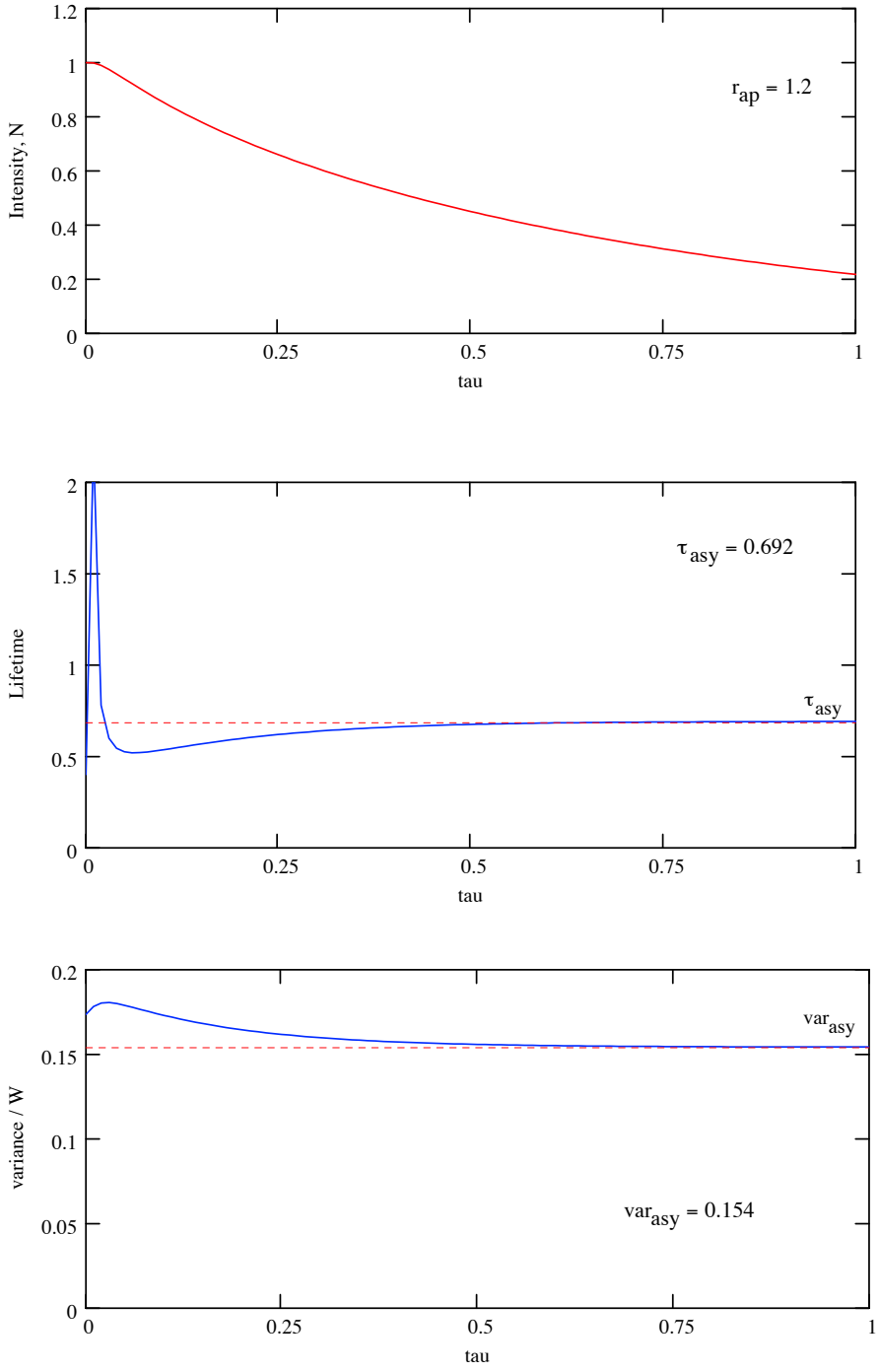

Figure 11: **Case (e) – Top to bottom: intensity N, lifetime τ_L, emittance $\langle x^2\rangle/W$ versus τ. Here, the initial beam distribution was uniform, out to $r = 5a/6$.**

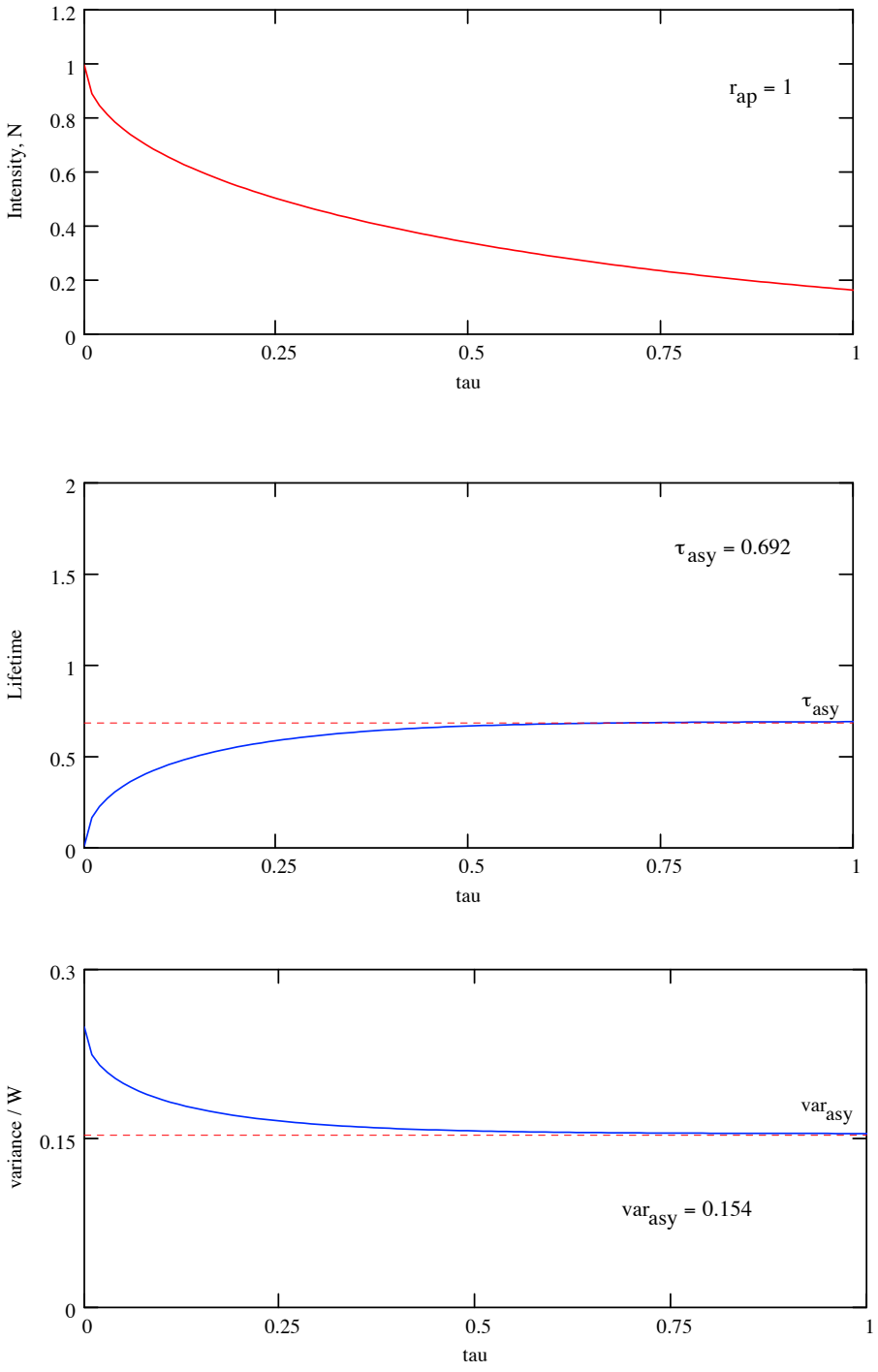

Figure 12: **Case (f) – Top to bottom: intensity N, lifetime τ_L, emittance $\langle x^2 \rangle / W$ versus τ. Here, the initial beam distribution was uniform, out to $r = a$.**

4.2 Application to the Tevatron at Injection

The purpose of Section 4 has been to get to a point where we could examine beam intensity versus time in the Tevatron and try to understand the relative roles of transverse and longitudinal diffusion mechanisms on the observed lifetimes. Prior to the last major shutdown, in late 2002 through 2003, as the intensity was raised in the Tevatron poor beam lifetimes were observed at injection. It was common for the proton beam intensity to fall over time with a "concave down" intensity curve, while often the antiproton beam's intensity curve would be "concave up." It was also shown in October 2002 that the antiproton beam intensity data over a half-hour period or so could be fit nicely to a "root-t" exponential function[4], $N \sim \exp(-\sqrt{t})$, as depicted in Figure 13, which was a temporary curiosity.

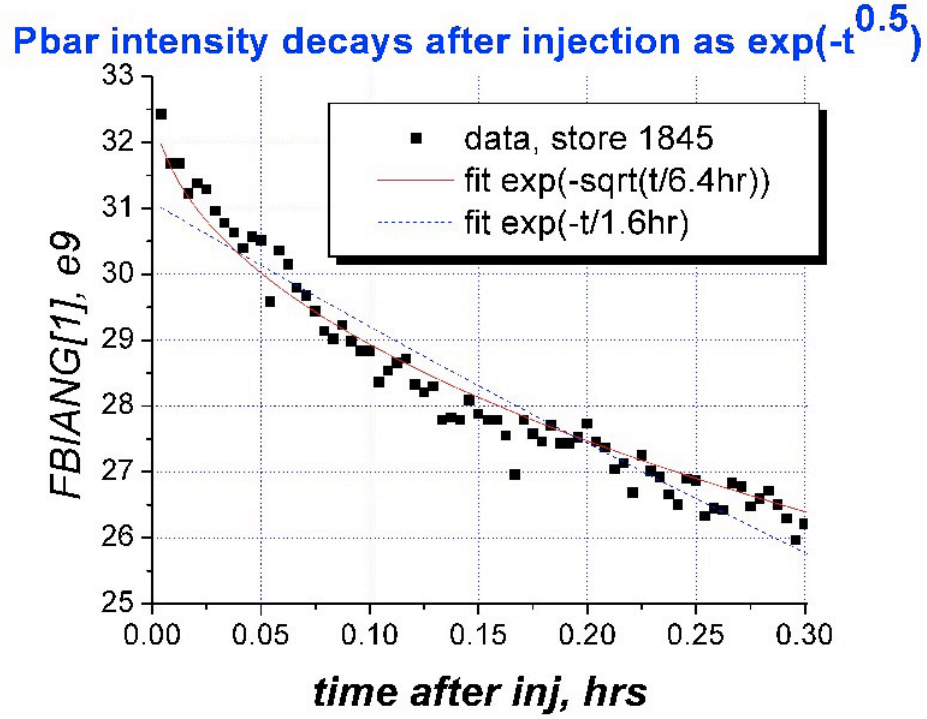

Figure 13: **Plot of antiproton intensity versus time for Collider Store 1845, indicating a "root-t" dependence. Courtesy V. Shiltsev.**

During the shutdown of Fall 2003, many improvements were made both to the Tevatron itself (magnet realignment, for example) as well as to the injector chain (such as the commissioning of the Main Injector longitudinal damper system) which resulted in increased aperture of the synchrotron and smaller injected beam size into the Tevatron. Since that shutdown the lifetime of both beam species has greatly improved. As illustrations of our above discussion, however, we will examine data from stores in late 2002.

In Figure 14 we show proton and antiproton intensity curves during two different Shot Set-ups

which were typical of conditions often encountered during that period. The proton curve is for Store 1971 which occured on 16 November 2002, while the antiproton curve is for Store 1886 taken 19 October 2002.[5] The proton beam behavior is indicative of the case where the emittance is just smaller than the admittance, whereas the antiproton beam behavior is more indicative of the case where the initial distribution is uniform out to the extent of the admittance of the accelerator. We

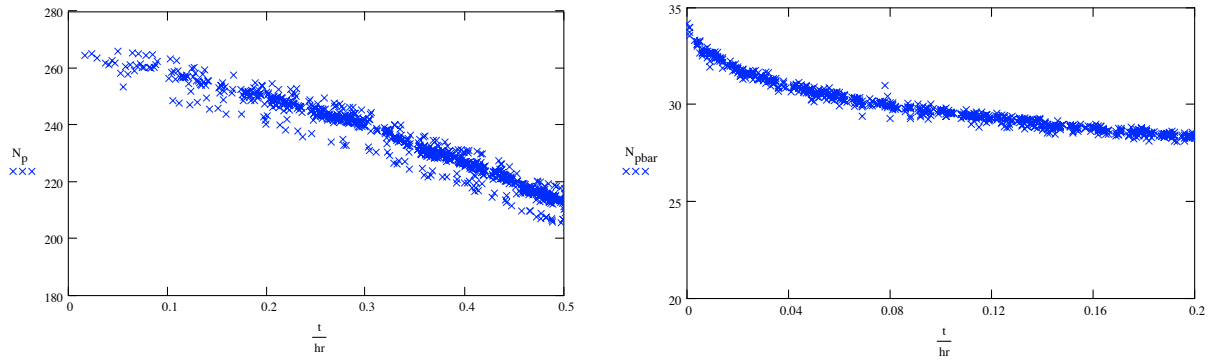

Figure 14: **Plot of proton (left) and antiproton (right) bunch intensity versus time for Collider Stores 1971 and 1886, respectively. Intensities are in units of** 10^9**.**

can now vary the major parameters of our diffusion problem to fit the solution $N(\tau)$ to the data. Namely, the time scale of the process is set by the ratio of W/R and the shape of the intensity evolution with time is set by the initial distribution function.

We examine the antiproton case first. It is indicative of a uniform distribution out to the admittance, and a time scale $0 < \tau < 0.03$ (corresponding to about 0.2 hr) fits well. The data are reproduced in Figure 15 as a function of τ along with the curve $N(\tau)$ for the aforementioned conditions.

For the other case, proton intensity during the set-up of Store 1971, we find that a Gaussian distribution with an aperture at about 3 σ_0 fits the data well, with the time scale corresponding to $t/\tau \approx 2$ hr. The data are re-plotted against τ in Figure 16.

The data above were taken from a very complicated environment, which includes long range beam-beam interactions, nonlinear magnetic fields encountered on the helical orbits, local transverse coupling, and various noise sources such as beam-gas interactions, RF and power supply noise, etc. While a simple diffusion model should not be expected to identify sources and cures, it may be enough to provide insights into possible leading mechanisms. For instance, the antiproton curve above seems to indicate a roughly uniform distribution out to a defining aperture. The transverse beam distribution for the antiprotons is known to be roughly Gaussian, due to the stochastic cooling process, and has relatively small transverse emittance. However, longitudinally, it would not be surprising for the distribution to be more uniform due to the multi-bunch coalescing process in the Main Injector prior to injection. If the defining aperture is the bucket, which we have seen has area $\mathcal{A} = 4$ eV-sec at injection, then we might wish to be looking for a longitudinal diffusion source

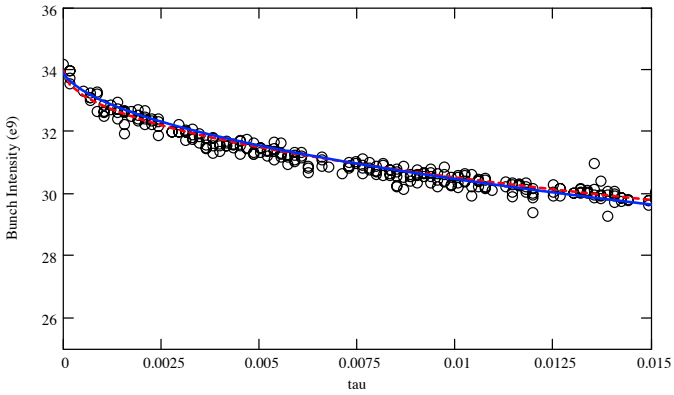

Figure 15: **Plot of antiproton intensity data versus τ for Collider Store 1886. Here, $t/\tau = W/R \approx$ 5.5 hr. Two curves are present also: $N(\tau)$ (solid) and $N_0 \exp(-\sqrt{\tau})$ (dashed) for an initial uniform distribution out to the admittance.**

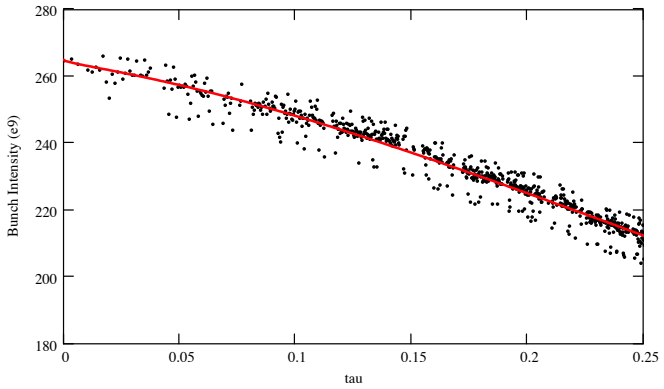

Figure 16: **Plot of proton intensity data versus τ for Collider Store 1971 along with the curve $N(\tau)$ for an initial distribution which is Gaussian out to an aperture at $a = 3\sigma_0$. Here, $t/\tau = W/R \approx$ 2 hr.**

which generates a growth rate of

$$\begin{aligned} d\langle x^2\rangle/dt &= R/2 = \frac{1}{2}\, W\, (\tau/t) \\ \longrightarrow \quad \dot{\epsilon_L} &\approx \frac{6}{2}\, (4 \text{ eV sec})\, (1/5.5 \text{ hr}) \approx 2 \text{ eV sec/hr} \end{aligned}$$

where the result is written in terms of the 95% emittance of a small amplitude particle. This example is not meant to draw any particular conclusion, but was meant to llustrate a route for examining the data.

5 exp(-$\sqrt{t}$)

To understand the "root-t" behavior, imagine a 2-D phase space which is uniformly filled with particles. Within a shell of thickness dr at a radius r, particles flow into and out of the shell due to a diffusion process. A particle's amplitude is changed on the n-th turn by a random process Δr_n, with $\langle \Delta r \rangle = 0$ and $\langle \Delta r^2 \rangle = (\Delta r_{rms})^2$. The rate of change of the particle amplitude variance with time will be $R \equiv f \Delta r_{rms}^2$, where f is the frequency of the random process. Thus, a particle with zero amplitude will develop a typical amplitude over time, $r \sim \sqrt{Rt}$ (a "random walk").

Now imagine the distribution exists out to a maximum radius a. The initial phase space particle density function is then $\rho = N/\pi a^2$. If we consider a ring of thickness dr at the maximum radius $r = a$, then during a short time step dt particle amplitudes will either grow or shrink, half of these being lost at the aperture. Thus, the initial rate at which particles are lost will be

$$\begin{aligned} \frac{dN}{dt} &= -\,\rho \cdot \left(2\pi a\, \frac{dr}{dt}\right) \cdot \frac{1}{2} = -\,\frac{N}{\pi a^2} \cdot 2\pi a\, \frac{dr}{dt} \cdot \frac{1}{2} = -\,\frac{N}{a}\, \frac{dr}{dt} \\ \rightarrow \quad \frac{dN}{N} &= -\,\frac{dr/dt}{a} = -\,\frac{1}{2}\frac{\sqrt{R}}{a}\, t^{-1/2} dt \\ \rightarrow \quad \ln N &= -\sqrt{\frac{R}{a^2}}\sqrt{t} + constant \\ \rightarrow \quad N &= N_0 e^{-\sqrt{Rt/a^2}} = N_0 e^{-\sqrt{Rt/W}} \\ &= N_0 e^{-\sqrt{\tau}}. \end{aligned}$$

Naturally, this "root-t" behavior will only occur during the initial onset of the beam loss. The diffusion will cause the distribution to change from a uniform distribution toward the equilibrium distribution found before. Eventually, the distribution will decay with its asymptotic lifetime. Figure 17 shows the result of a simulation of an initially uniform distribution decaying due to diffusion. For small values of τ, $N(\tau) \sim \exp(-\sqrt{\tau})$; by $\tau \sim 1$ we see $N(\tau) \sim \exp(-\tau/\tau_L^{\infty})$.

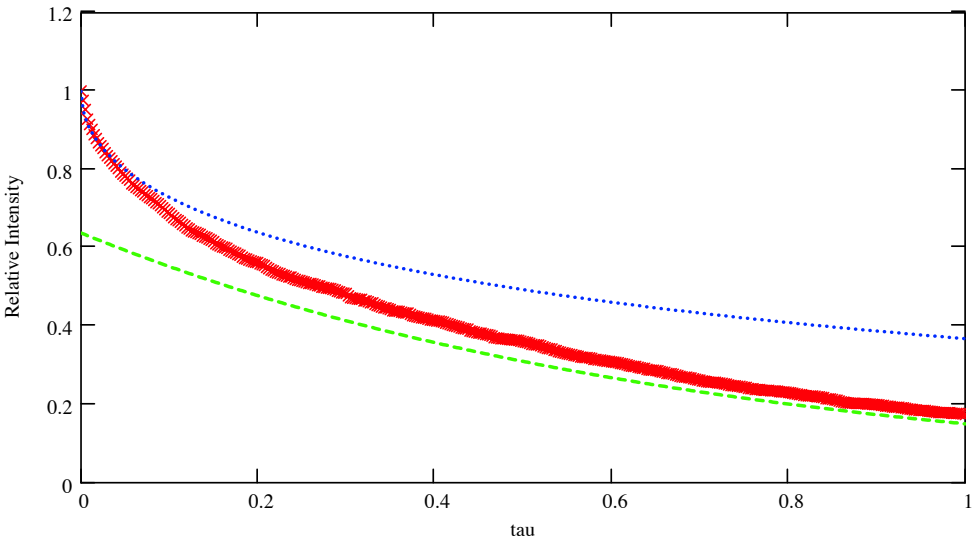

Figure 17: **Result of a diffusion simulation with initial uniform phase space distribution of 2000 particles. The upper dotted curve is the function** $\exp(-\sqrt{\tau})$ **while the lower dotted curve is the function** $b_1 \cdot \exp(-\tau/\tau_L^\infty)$**, where** $\tau_L^\infty = 4/\lambda_1^2$**. The coefficient** b_1 **is the coefficient of the first term of the infinite series given in Equation 6.**

6 Concluding Remarks

The purpose of this note was to explain the general mechanics of simple diffusion and to illustrate what might be observed from the Main Control Room during routine operation of the Tevatron. The Shot Data Analysis (SDA) package provides opportunities for systematic studies of emittance growth rates, beam lifetimes, and equilibrium admittance measurements, hopefully leading toward the discoveries of causes and cures. It is also hoped that the role of longitudinal effects on the observed beam lifetimes in the Tevatron can be better appreciated by the reader.

References

[1] D. Edwards and M. Syphers, *An Introduction to the Physics of High Energy Accelerators*, Wiley & Sons, Inc., New York (1993).

[2] See, for example, C.Y. Tan, "A method for calculating longitudinal phase space distribution when given the time profile of the bunch," Fermilab-TM-2155 (2001); L. Michelotti, "An integral for longitudinal phase space tomography on equilibrium distributions," Fermilab-FN-0726 (2002); A. Tollestrup, "A simple numerical algorithm for obtaining longitudinal phase space density from the time projection of the current," Beams-doc-548 (2003).

[3] See, for example, R. Gerig, et al., "Main Ring Dynamic Aperture Studies," Fermilab Report EXP-164 (1989).

[4] V. Shiltsev, private communication, 18 October 2002.

[5] Data courtesy P. Le Brun, private communication.